Liquid Crystals
Publication details, including instructions for authors and subscription information:
http://www.informaworld.com/smpp/title~content=t713926090

Pretilt study of double-layer alignment film (DLAF)

Ke Zhang[a]; Na Liu[b]; Robert J. Twieg[b]; Brian C. Auman[c]; Philip J. Bos[a]
[a] Liquid Crystal Institute, Kent State University, Kent, OH 44242 [b] Chemistry Department, Kent State University, Kent, OH 44242 [c] Circleville Research Laboratory, DuPont Electronic Technologies, Circleville, OH 43113

To cite this Article Zhang, Ke , Liu, Na , Twieg, Robert J. , Auman, Brian C. and Bos, Philip J.(2008) 'Pretilt study of double-layer alignment film (DLAF)', Liquid Crystals, 35: 10, 1191 — 1197
To link to this Article: DOI: 10.1080/02678290802444103
URL: http://dx.doi.org/10.1080/02678290802444103

Liquid Crystals,
Vol. 35, No. 10, October 2008, 1191–1197

Taylor & Francis
Taylor & Francis Group

Pretilt study of double-layer alignment film (DLAF)

Ke Zhang[a], Na Liu[b], Robert J. Twieg[b], Brian C. Auman[c] and Philip J. Bos[a]*

[a]*Liquid Crystal Institute, Kent State University, Kent, OH 44242, USA;* [b]*Chemistry Department, Kent State University, Kent, OH 44242, USA;* [c]*Circleville Research Laboratory, DuPont Electronic Technologies, Circleville, OH 43113, USA*

(Received 6 June 2008; final form 1 September 2008)

A novel double-layer alignment film (DLAF) was developed to obtain greater control of the alignment characteristics of the liquid crystal director. The DLAF consists of a thin fluorinated polymer layer on the top of a rubbed non-fluorinated, non-branched polyimide layer (PI 2555). Two types of fluorinated polymer with different chemical structures and wetting behaviour on PI 2555 were chosen, to provide either continuous or discontinuous top layers. The continuous top layer DLAF (DLAF-1) exhibits an abrupt pretilt transition from planar to homeotropic as the top layer thickness increases. The discontinuous top layer DLAF (DLAF-2) exhibits a gradual transition where the pretilt correlates with the coverage of fluorinated top layer. These two types of transitions fit with de Gennes' local Frederick's transition and Kwok's inhomogeneous alignment theories, respectively. The abrupt pretilt transition system may be promising for chemical/biosensor applications, whereas the gradual transition system is suitable for pretilt control in LCD devices.

Keywords: alignment; liquid crystal display; pretilt; double-layer alignment film; sensor

1. Introduction

Alignment films are one of the most important components in liquid crystal (LC) devices. These films are usually composed of an anisotropic material (e.g. rubbed, stretched, photoaligned, evaporated thin film, surfactant layer, etc), which influences LC molecules to preferably align in a certain direction through van der Waals forces, dipolar interactions, steric interactions, etc. (*1*). As an electric field switches the LC away from the state defined by the alignment film, a change in optical response is produced. This interaction between the electric field and the liquid crystal is the general principle for the operation of most LC display devices. An important parameter for characterisation of an alignment film is the pretilt angle, which is the angle between the LC director and the film plane.

As LCs become increasingly important for display, telecom and biological applications, more complete control of alignment characteristics of the LC director would be advantageous. Many research groups have investigated homogeneous alignment layers, such as common polyimides, but it has proved difficult to control certain characteristics of the director alignment. For example, control of an anchoring transition for bistable devices and sensors, or control of the pretilt over the entire angular range from 0 to 90°, are both difficult to achieve.

Another method for pretilt control involves the use of a *heterogeneous* alignment film, wherein the alignment of LC molecules results from the averaged interaction of regions that provide a different alignment preference. An example is a multilayer film proposed by Dubois-Violette and de Gennes (*2*) and Hinov (*3*) who predicted a ''local Frederick's transition'' of LC alignment on a crystalline surface covered with a thin amorphous film. The crystalline substrates considered imposed planar alignment of LCs via long range van de Waals forces, whereas a short-range interaction between the LC and the top amorphous film favoured homeotropic alignment. Later, Blinov and Sonin observed the anchoring transition of MBBA on a Langmuir–Blodgett film coated mica surface (*4, 5*). They found an abrupt planar to homeotropic anchoring transition as the LB film thickness increases. We denote this as a Type I pretilt transition.

In contrast to the continuous layers, a spatially heterogeneous single layer alignment film has recently been investigated for example by Kwok and co-workers (*6, 7*) for 0 to 90° pretilt control. They mixed commercial vertical and planar aligning polyimides (PIs) and obtained thin films with a spatially uniform microphase separation. On the vertical/planar PI enriched domains the LC molecules align vertically/planarly. The LC director acquires an averaged pretilt in the bulk. The pretilt value is determined by the area ratio and the anchoring energy difference between the two PIs. As the area ratio is changed this pretilt transition is much more gradual than the abrupt Type I pretilt transition, and is denoted here as a Type II pretilt transition.

*Corresponding author. Email: pbos@lci.kent.edu

ISSN 0267-8292 print/ISSN 1366-5855 online

DOI: 10.1080/02678290802444103
http://www.informaworld.com

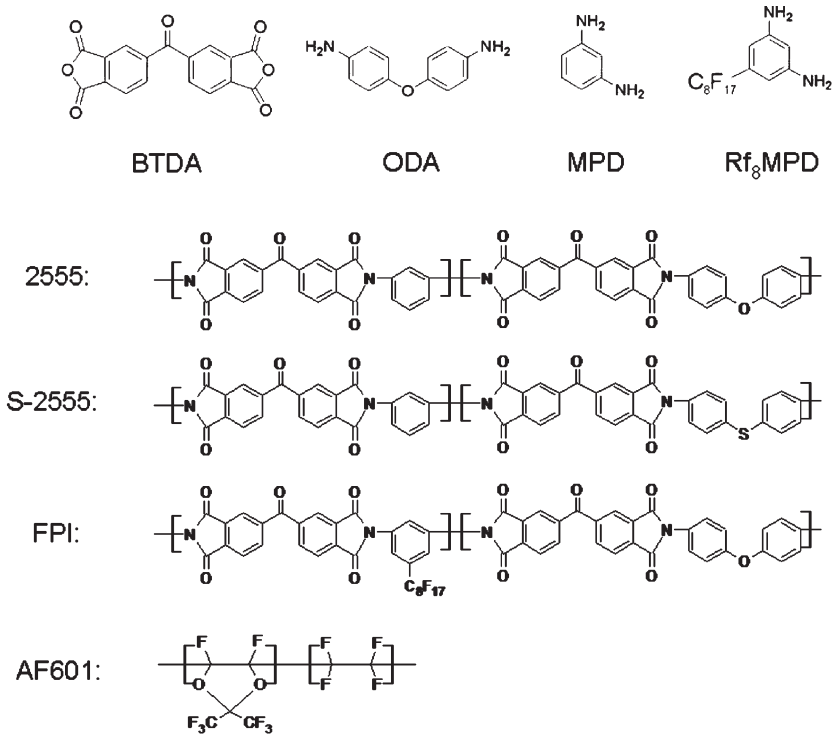

Figure 1. The chemical structures of the polymers and some of their monomer components used in this study.

In this paper, we focus on tuning the alignment film structure to control the pretilt behaviour. Here we introduce a novel double-layer alignment film (DLAF) method to realise both Type I and Type II transitions. More specifically, we first coat the substrate with a regular main-chain polymer that provides strong planar alignment. Next, one of two fluorinated polymer materials is chosen as the top layer to create Type I and Type II pretilt control, respectively. We call these corresponding two types of alignment layers DLAF-1 and DLAF-2 and we will show that our DLAF-1 alignment films have a continuous top layer of a fluorinated polymer, and our DLAF-2 alignment films have a discontinuous top layer of a fluorinated polymer.

2. Experimental

Material and sample preparation

To achieve a wide range of pretilt control, we chose planar and homeotropic alignment materials for the bottom and top layers, respectively. For the bottom layer, we used Pyralin 2555, which is a copolymer made from benzophenone tetracarboxylic dianhydride (BTDA) and a mixture of the two diamines, 4,4′-oxydianiline (ODA) and *m*-phenylenediamine (MPD). The structures of the monomers and the polymers used are shown in Figure 1.

For the top layer, we chose two kinds of fluorinated polymer. One (for DLAF-1) is the fluorinated polyimide (FPI) (*8*) shown in Figure 1. The heavily fluorinated side chains on the FPI may be expected to preferentially reside on the surface owing to their low polarisabilty, and serve as a source of low surface tension, which favours homeotropic alignment of LC molecules (*9*). The backbone structure for this polyimide is similar to that found in 2555 (shown in Figure 1) so as to promote wetting and the formation of the uniform double layer structures, which are required for Type I pretilt control. For the top layer of DLAF-2 we used the commercial fluorinated polymer, AF601. It is a copolymer of 4,5-difluoro-2,2-bis(trifluoromethyl)-1,3-dioxole and tetrafluoroethlyene (Figure 1). Judging from their chemical structures, AF601 is anticipated to dewet on the 2555, and lead to a heterogeneous surface for Type II pretilt transition.

Synthesis of polyamic acid (PAA) of FPI.

The precursors BTDA, ODA and MPD were purchased from Sigma-Aldrich and purified by recrystallisation or sublimation. The synthesis protocol for fluorinated PAA (F-PAA) is described elsewhere (*8*). Typically, 1.843 g (5.72 mmol) BTDA, 0.573 g (2.86 mmol) ODA and 1.382 g (2.86 mmol) MPD (*8*) were charged to a 100 ml reaction kettle.

N-Methyl-2-pyrrolidone (NMP, 20.5 ml) was added to dissolve the monomers and the polymerisation was allowed to proceed. The solvent volume was adjusted to a give ~16% solids concentration. The reaction was carried out under nitrogen protection and with good stirring overnight (~16 h) at room temperature. The PAA is produced as a viscous brownish solution and was stored at −5°C for future use.

Introducing sulfur-tagged 2555 (S-2555) for XPS characterisation.

Since 2555 and FPI share similar structure and elemental composition, one cannot differentiate the signals from the bottom layer by XPS analysis. Therefore, we substituted the ODA in Pyralin 2555 with 4,4′-thiodianiline (TDA) in order to introduce sulfur in the main-chain polymer to provide an exclusive XPS signal from the bottom layer. The synthesis of the PAA of S-2555 follows the same protocol as for F-PAA described above, except the precursors are BTDA, TDA and MPD in the mol ratios of 2:1:1. Due to the substitution of sulfur, the S-2555 PAA appears much darker than 2555. The S-2555 could be coated as continuous film and it was tested to provide strong planar alignment after rubbing.

Fabrication of DLAF.

The F-PAA solution (16% solid concentration) was warmed to room temperature and diluted with NMP immediately before spin-coating. To achieve different film thickness, the F-PAA was diluted to a variety of solid concentrations (from 0.1% to 4% by weight). After mechanical homogenisation with a Vortex Genie 2, the diluted F-PAA solution was ready to spin-coat. The DuPont 2555 polyamic acid (purchased from HD MicroSystems) had a 20% solids concentration. It was diluted to 4% solids concentration using NMP immediately before spin-coating.

The ITO substrates were cleaned in an ultrasonic cleaner (Branson) and thoroughly rinsed with deionised water and isopropanol. After drying in an oven (80°C, 20 min), the substrates were first spin-coated with 2555 at 2500 rpm for 20 s. The coated substrates were soft baked at 90°C for 90 s to evaporate most of the solvent, followed by a hard bake at 300°C for 1 h to complete the imidisation reaction. Next, the 2555-coated substrates were rubbed using a velvet cloth to produce a strong planar alignment. After rubbing, F-PAA was spin-coated on the top of the 2555 at 2500 rpm for 20 s, and then soft baked at 90°C for 90 s. The substrates with a double layer coating were baked in the oven following this protocol: keep at 90°C for 15 min; ramp to 260°C over one hour; keep at 260°C for 30 min; and finally cool down to room temperature in an hour. This process completed the imidisation of F-PAA to FPI. This DLAF with an FPI on the top of 2555 was labelled DLAF-1. The DLAF-2 was fabricated following the same process, but substituting the F-PAA with an AF601 solution. The original AF601 (amorphous fluoropolymer, from Du Pont) contains 6 wt % fluoropolymer in a C5-18 fluorocarbon solvent. Prior to spin-coating, AF601 was further diluted to a variety of solid concentrations using the fluorocarbon solvent FC40 (Fluorinert fluids, from 3M). The fabrication processes for the two types of DLAF are illustrated in Figure 2.

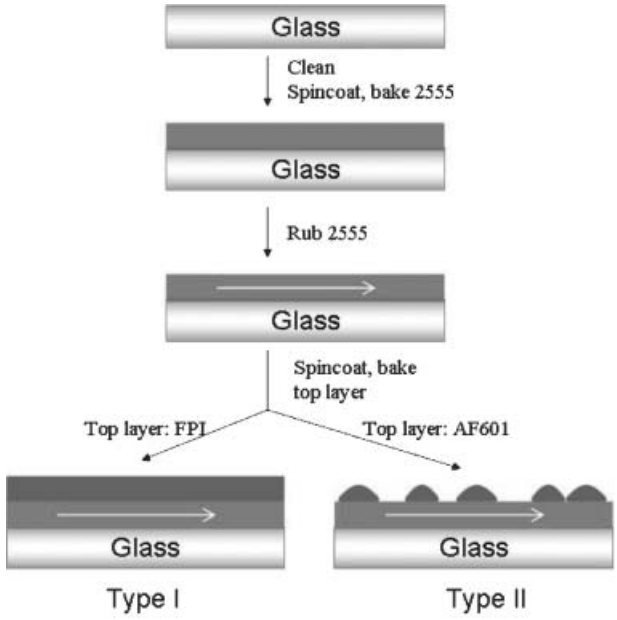

Figure 2. Structure and fabrication processes for two types of DLAFs (the white arrows in the layers indicate that they have been rubbed).

Cell assembly.

The DLAF coated substrates were assembled into 16 μm thick sandwich cells with antiparallel rubbing directions between the top and bottom plates. The LC ZLI 2293 (purchased from EM chemicals and used without further treatment) was capillary filled into the cells at room temperature. The filled cells were heated to 100°C (above the clearing point of 85°C for ZLI 2293) and kept for 10 min before slowly cooling back to room temperature.

Characterisation techniques

Atomic force microscopy (AFM) and X-ray photoelectron spectroscopy (XPS) were employed to

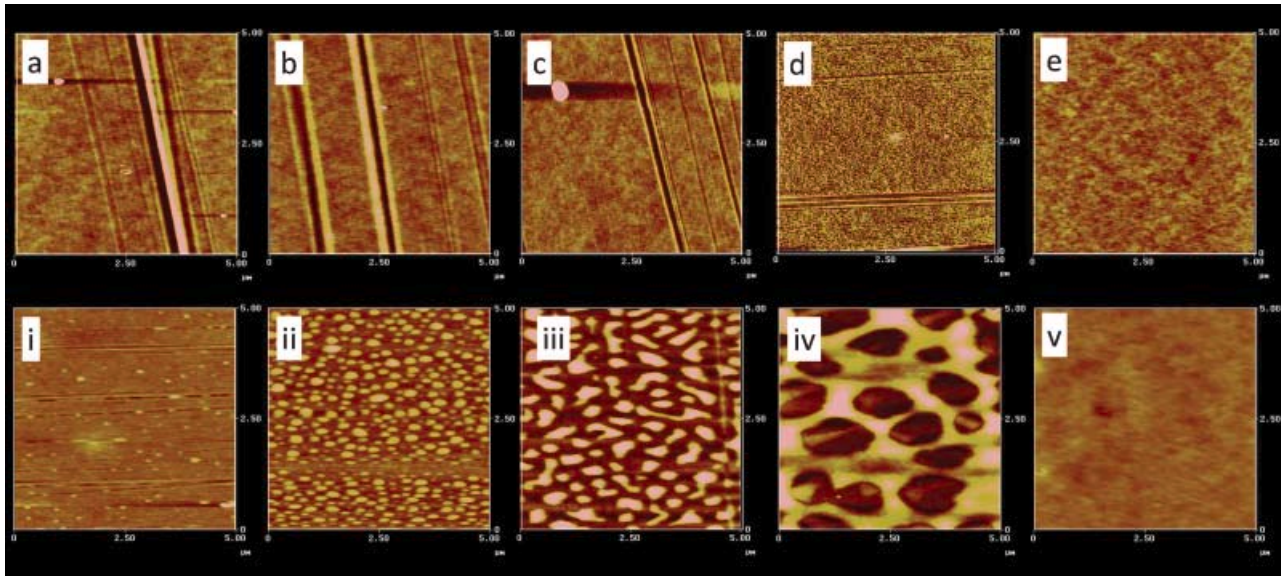

Figure 3. AFM pictures of two DLAF: top row (a–e) are DLAF-1 with top layer solids concentration of 0.1%, 0.2%, 0.4%, 0.5% and 4%; bottom row (i–v) are DLAF-2 with top layer solids concentration of 0.06%, 0.1%, 0.2%, 0.3% and 0.4%.

characterise the DLAF structure and composition. For the XPS studies, the S-2555 replaced 2555 in the DLAF to provide an exclusive XPS signal due to sulfur from the bottom layer. The pretilt angles of the LC test cells assembled with DLAF substrates were measured using the magnetic null method (*10*).

3. Results

Film structure study of DLAF by AFM and XPS

The AFM studies suggest distinctive film structures for the two types of DLAF. The AFM pictures in Figure 3 are all configured to have the same dimensions and colour-coding. As all the substrates have the bottom layer rubbed, some grooves can be seen in the AFM pictures, and they become less obvious as the top layer solids concentration increases. It is clear that DLAF-1 shows a uniform top layer while DLAF-2 exhibits a clear dewetting behaviour. From left to right in the bottom row of Figure 3, one can see the isolated bright islands (corresponding to AF601) increasing in domain size and coverage as the solids concentration increases. At 0.3%, it changes to a continuous phase and the dark region (corresponding to 2555) is dispersed. When further increased to 0.4%, the AF601 covers the entire surface. The difference in the film structure results from the contrast in chemical structures of the two layers, as discussed previously.

Another observation in some DLAF-2 films is that dewetted islands are slightly elongated along the rubbing direction of the bottom 2555 layer (e.g. Figure 3ii). It is well known that liquid crystals can be aligned by obliquely evaporated SiO_x (*11*) and micro/nano grooves through topological interaction (*12–14*). In order to evaluate the contribution of the topography to the pretilt, we further examined the morphology of the DLAF-2 films. The sectioned view of the islands along the rubbing direction shows a symmetric shape (see Figure 4), which is unlikely to induce a preference in pretilt (unlike the obliquely evaporated SiO_x, where the SiO_x columns are clearly tilted). We also found, in the most anisotropic case, the dimensions of the islands are ~10 nm in height, ~100 nm in width and ~200 nm in length. This topography might affect the azimuthal anchoring, but not zenithal anchoring (pretilt).

To obtain more conclusive information about the film structures, we further studied the DLAFs with XPS. The fluorine signal from the top layer (FPI or AF601) and the sulfur signal from the bottom layer (S-2555) are ideal to analyse the double layer film structures. Considering the case of a continuous top layer (DLAF-1), the XPS signal from the bottom layer (I_B) was attenuated by passage through the top layer. According to the Beer–Lambert law, this intensity decays exponentially as the top layer thickness (d_T) increases, i.e. $I_B \propto \exp(-d_T/\lambda_{TB})$, where λ_{TB} is the attenuation length in the top layer for the electrons emitted from the bottom layer. Meanwhile, the top layer signal (I_T) decreases as its thickness gets smaller as $I_T \propto 1-\exp(-d_T/\lambda_{TT})$, where λ_{TT} is the attenuation length of its own electrons within the layer. The ratio of signals from the top to the bottom layer becomes $I_T/I_B \propto \exp(d_T/\lambda_{TB})\left[1-\exp\left(\frac{k-1}{k}\right)\right]$, where k is ratio of attenuation lengths $\lambda_{TT}/\lambda_{TB}$. As k is a constant, the ratio I_T/I_B, in our case F/S, should

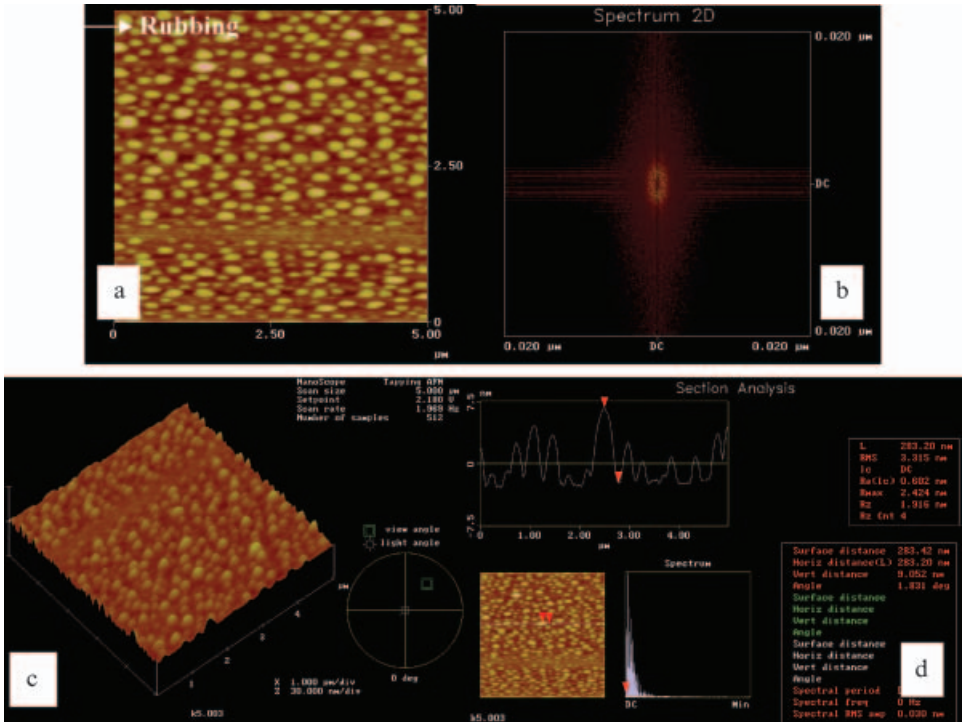

Figure 4. AFM study on one of the DLAF-2 films with most pronounced anisotropy: (a) height profile; (b) 2D-FFT analysis; (c) 3D image; (d) section analysis along the rubbing direction.

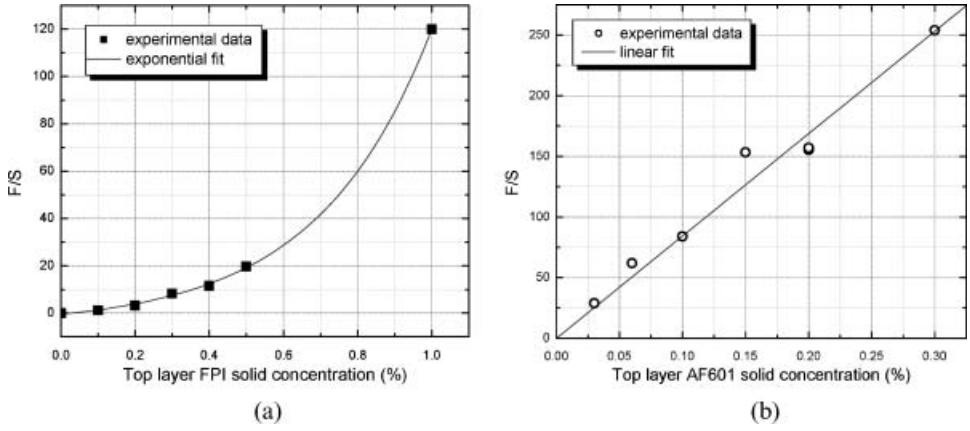

Figure 5. Relationship between the ratio of F 1s (bottom layer) to S 2s (top layer) XPS signals and the top layer solids concentration of DLAF-1 (a) and DLAF-2 (b).

follow an exponential growth as the top layer thickness increases (*6, 15*). On the other hand, if the top layer is not continuous, the bottom layer signal can be detected without ever passing through the top layer. The ratio I_T/I_B is proportional to the area ratio of the two materials, which should linearly increase with the top layer solid concentration until top layer become continuous and thick enough to screen the signal from the bottom layer.

Our XPS data (Figure 5) exactly demonstrated these two cases. The DLAF-1 data follow an exponential growth relative to the FPI solid concentration, which complies with the continuous top layer situation. At low concentration, 0–0.5%, it seems the data might follow a linear pattern. However, the linear fits in 0–0.5%, 0–0.4% and 0–0.3% all results lower correlation coefficients than the exponential fits (see Table 1). We believe DLAF-1 is always a continuous top layer structure even at low concentrations. This agrees with the AFM results where only a flat surface is observed for all the FPI samples. In contrast, the DLAF-2 data demonstrate a typical linear relationship and in agreement with the dewetting effect from the AFM

Table 1. Fitting correlation coefficients of XPS signal ratio F 1s to S 2s for DLAF-1.

Data range		0–1%	0–0.5%	0~0.4%	0–0.3%
Fitting correlation coefficient, R^2	Exponential fit	0.99979	0.99946	0.99862	0.99995
	Linear fit	0.90062	0.90402	0.94228	0.98470

study. The XPS data also serve as a good measure for the area ratio of the sample with a discontinuous top layer.

Pretilt study of two types of DLAF

We found that a single layer of AF601 and FPI both gave homeotropic alignment without rubbing. Therefore, for the case of DLAF, we should obtain planar alignment when the top layer concentration is ~0 (just as for a 2555 single layer), and homeotropic alignment when the top layer is continuous and thick enough to shield any influence from the bottom layer, and essentially be treated as a single layer alignment film. This agrees with our results (see Figure 6). What is more interesting is how the pretilt varies in between these two extreme cases. As shown in Figure 6, for DLAF-2, the pretilt gradually shifts from planar to homeotropic with an increase of solids concentration. In contrast, DLAF-1 gives an abrupt switch from planar to homeotropic almost without any intermediate states as a function of the thickness of the top layer. We have clearly demonstrated Type I and Type II pretilt transition using DLAF-1 and DLAF-2, respectively.

4. Discussion

As Kwok and co-workers (*7*) pointed out, the pretilt of an inhomogeneous surface composed of planar and homeotropic domains results from the averaging effect of local alignment of LCs. The value of the pretilt is determined by the anchoring energy ratio and the area ratio of the homeotropic to planar region. Our DLAF-2 system fits in this theory quite nicely. Our method using the dewetting process helps to provide clean domain boundaries between the planar and homeotropic regions. The solid concentration of the spin coating solution is a very efficient dial for precise control of the area ratio. The convenient spin-coating procedure is highly compatible with current alignment film fabrication processes.

As for the DLAF-1 layer that shows the Type 1 transition, we can apply the ''local Frederick's transition'' theory of Dubois-Violette and de Gennes, the bottom layer and top layer both affect the LC alignment. However, the top layer screens the van der Waals interaction from the bottom layer. The dispersion potential diminishes as d^3, where d is the top layer thickness. This leads to an abrupt transition of the pretilt angle vs. d. The Type I pretilt change in DLAF-1 type films could be very attractive for sensor applications. The presence of trace quantities of analyte may trigger the pretilt transition, which, in turn, produces a macroscopic optical signal that can be easily detected.

The DLAF structure is determined by the chemical miscibility of the top and bottom polymer films as well as the spin-coating process that produces them. With complete information on chemical structures, we are able to tune the film structures to control the pretilt behaviour. The DLAF-1 and DLAF-2 examples are two extreme cases to clearly demonstrate the influence of miscibility. When the top layer material has a miscibility between FPI and AF601, the resulting

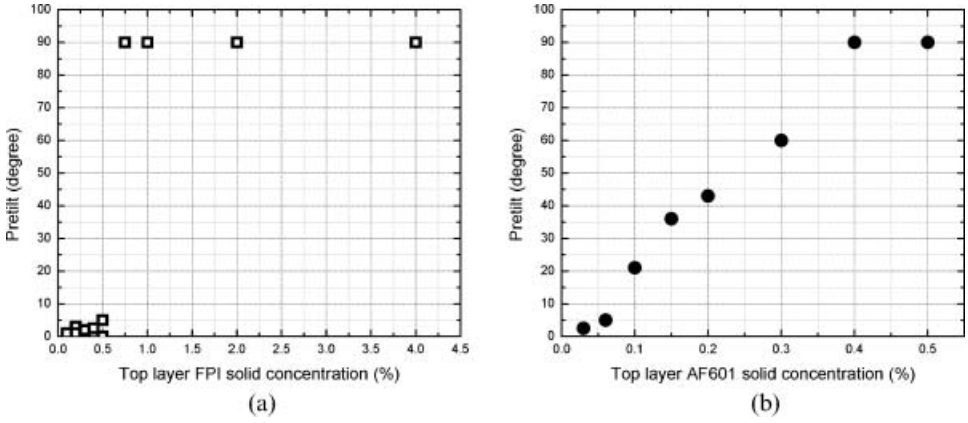

Figure 6. Pretilt dependence on the solid concentration of the top layers of DLAF-1 (a) and DLAF-2 (b).

DLAF might be in an intermediate state between two uniform layers or a dewetted top layer structure, which might affect the pretilt in a more complicated way. On the other hand, the spin-coating conditions have a major influence on properties of the resulting film. So, the factors like the boiling point of the spin-coating solvent, spin-coating speed and duration may change the top layer morphology significantly. Further investigation of the alignment behavior of these DLAFs is currently underway.

5. Conclusions

We have designed and observed two distinctive pretilt manipulating behaviours using two types of DLAF with different film structures. The DLAF-1 system gives an abrupt transition from planar to homeotropic as the film thickness increases. This phenomenon can be explained by the Dubois-Violette and de Gennes "local Frederick's transition" theory. This abrupt switch of LC alignment is promising for sensor applications when an extremely low concentration of reagent can trigger a dramatic pretilt change producing a macroscopic optical signal. The DLAF-2 system offers a more graduated transition, which agrees with Kwok's theory. Here, the pretilt is the average effect of local alignment on homeotropic and vertical domains. DLAF-2 is interesting for display applications such as in STN and SmC* devices, where a stable intermediate pretilt angle is crucial, and is otherwise difficult to realise using single layer organic materials.

Acknowledgements

This work was supported by DuPont. The authors would like to thank Fenghua Li at the Liquid Crystal Institute for characterisation of the properties of fluorinated polyimide materials; Liou Qiu, Sergij Shiyanoviskii, and Rui Guo at the Liquid Crystal Institute for AFM analysis; Wayne Jennings at Case Western Reserve University for the XPS study; and David Stiff at 3M company for providing FC samples.

References

(1) Takatoh K.; Hasegawa M.; Koden M.; Itoh N.; Hasegawa R.; Sakamoto M. *Alignment Technologies and Applications of Liquid Crystal Devices*; Taylor & Francis: London, 2005.
(2) Dubois-Violette E.; de Gennes P.G. *J. Colloid Interface Sci.* **1976**, *57*, 403–410.
(3) Hinov H.P. *J. Phys. Lett., Paris* **1977**, *38*, 215–219.
(4) Sonin A.A. *The Surface Physics of Liquid Crystals;* Gordon and Breach: 1995.
(5) Blinov L.M.; Sonin A.A. *Mol. Cryst. Liq. Cryst. Sci.* **1990**, *179*, 13–25.
(6) Wan J.T.K.; Tsui O.K.C.; Kwok H.-S.; Sheng P. *Phys. Rev. E* **2005**, *72*, 021711/1–4.
(7) Yeung F.S.; Ho J.Y.; Li Y.W.; Xie F.C.; Tsui O.K.; Sheng P.; Kwok H.S. *Appl. Phys. Lett.* **2006**, *88*, 051910/1–3.
(8) Estes W.E.; Higley D.P.; Auman B.C.; Feiring A.E. Liquid Crystal Displays of High Tilt Bias Angles. US Patent 5,186,985, February 19. 1993.
(9) Creagh L.T.; Kmetz A.R. *Mol. Cryst. Liq. Cryst. Sci.* **1973**, *24*, 59–68.
(10) Scheffer T.J.; Nehring J. *J. Appl. Phys.* **1977**, *48*, 1783–1792.
(11) Janning J.L. *Appl. Phys. Lett.* **1972**, *21*, 173–174.
(12) Ibn-Elhaj M.; Schadt M. *Jap. J. Appl. Phys.* **2003**, *42*, 6896–6909.
(13) Ruetschi M.; Grutter P.; Funfschilling J.; Guntherodt H.J. *Science* **1994**, *265*, 512–514.
(14) Kim M.-H.; Kim J.-D.; Fukuda T.; Matsuda H. *Liq. Cryst.* **2000**, *27*, 1633–1640.
(15) Watts J.F.; Wolstenholme J. *An Introduction to Surface Analysis by XPS and AES*; J. Wiley: New York, 2003.